# METTL3 mediates m6A modification of lncRNA *CRNDE* to promote *ATG10* expression and improve brain ischemia/ reperfusion injury through YTHDC1

Zhengtao Yu[1], Ying Xia[1], Jiameng Li[1], Junwen Jiang[1], You Li[1], Youjun Li[1*] and Liu Wang[2*]

## Abstract

**Background**  Ischemia/reperfusion (I/R) injury is a severe brain disorder with currently limited effective treatments. This study aims to explore the role of N6-methyladenosine (m6A) modification and associated regulatory factors in I/R to identify potential therapeutic targets.

**Methods**  We utilized a middle cerebral artery occlusion (MCAO) rat model and SH-SY5Y cells subjected to oxygen-glucose deprivation/reoxygenation (OGD/R) to assess m6A levels and investigate the impact of *METTL3* overexpression on long non-coding RNA (lncRNA) *CRNDE* expression. The effects of silencing lncRNA *CRNDE* on the interaction between YTHDC1 and *ATG10* mRNA, as well as the stability of *ATG10* mRNA, were evaluated. Additionally, apoptosis rates, pro-inflammatory and anti-inflammatory factor levels, *ATG10* expression, and autophagic activity were analyzed to determine the effects of *METTL3*. The reverse effects of *YTHDC1* overexpression were also examined.

**Results**  MCAO rats and OGD/R-treated SH-SY5Y cells exhibited reduced m6A levels. *METTL3* overexpression significantly inhibited lncRNA *CRNDE* expression. Silencing lncRNA *CRNDE* mitigated OGD/R-induced apoptosis and inflammation in SH-SY5Y cells, while enhancing autophagy and stabilizing *ATG10* mRNA. *METTL3* overexpression decreased cell apoptosis, reduced the levels of pro-inflammatory cytokines TNF-α, IL-1β, IL-6, and increased IL-10 secretion. Furthermore, *METTL3* overexpression upregulated *ATG10* expression and promoted autophagy. Conversely, lncRNA *CRNDE* overexpression negated these effects.

**Conclusion**  The inhibition of lncRNA *CRNDE* affects the interaction between YTHDC1 and *ATG10* mRNA and stabilizes *ATG10* mRNA, mediated by *METTL3* overexpression. These findings suggest that targeting lncRNA *CRNDE* to reduce apoptosis, inhibit inflammation, increase *ATG10* expression, and enhance autophagy could offer new therapeutic strategies for I/R injury.

**Keywords**  METTL3, YTHDC1, *ATG10*, m6A, lncRNA *CRNDE*, Ischemia/reperfusion

*Correspondence:
Youjun Li
596111156@qq.com
Liu Wang
wangliu610@163.com

[1]Department of Neurosurgery, Haikou People's Hospital and Haikou Affiliated Hospital of Xiangya School of Medicine, Central South University, Haikou, Hainan, China
[2]Phase I Clinical Trial Center, Haikou People's Hospital and Haikou Affiliated Hospital of Xiangya School of Medicine, Central South University, Haikou, Hainan, China

## Introduction

Acute ischemic stroke (AIS) is a severe neurological disorder characterized by high incidence, substantial disability, and significant mortality, leading to considerable psychological and economic burdens on patients and society [1]. The primary treatments for AIS are intravenous administration of recombinant tissue plasminogen activator (tPA) and endovascular thrombectomy (EVT) [2]. However, the narrow treatment window limits the effectiveness of these therapies, leaving many AIS patients without viable acute treatment options [3]. Cerebral ischemia-reperfusion (I/R) injury can trigger various forms of programmed cell death, including neuronal apoptosis, autophagy, and necroptosis, which are often inevitable and irreversible [4]. Thus, enhancing neuronal resistance to ischemic conditions is essential, especially in the early stages of AIS when neurons with mild damage have not yet progressed to apoptosis or necrosis.

Epigenetic transcriptomics, the study of RNA modifications, has revealed that these modifications play significant roles in the pathophysiology of various diseases [5]. More than 170 types of RNA modifications have been identified, with N6-methyladenosine (m6A) being the most prevalent and widespread in eukaryotes, particularly in the mammalian brain [6]. m6A modification of mRNA is dynamic and reversible, regulated by the methyltransferase *METTL3* and demethylases such as Fat mass and obesity-associated (FTO) and AlkB homolog 5 (ALKBH5) [7, 8]. The differential expression of m6A levels influences numerous biological processes, including selective splicing of transcripts, nuclear RNA export, protein translation, heat shock response, cell fate determination, meiosis, and cardiac function [9]. Recent study indicated that m6A-related enzymes are crucial in ischemic diseases. *METTL3*, for instance, has been shown to regulate axonal regeneration, neuronal apoptosis, neurogenesis, and inflammation following cerebral ischemia [10]. These findings suggested that m6A modification may play a significant role in the molecular events occurring after stroke.

Long non-coding RNAs (lncRNAs) are non-coding transcripts longer than 200 nucleotides in length that lack protein-coding potential [11]. Evidence increasingly supports the role of lncRNAs as novel gene expression regulators, essential for various biological processes including the cell cycle, differentiation, epigenetic regulation, and tissue homeostasis [12]. Dysregulated lncRNA expression is associated with numerous diseases, ranging from neurodegenerative disorders to cancer. The complex gene regulatory mechanisms underscore the need for both stability and adaptability in neuronal signaling [13]. Recent studies, both in vivo and in vitro, have highlighted the involvement of m6A modification in brain ischemia-reperfusion injury, demonstrating that inhibition of m6A methylation can protect neurons from ischemia-reperfusion damage [14]. m6A modification regulates lncRNA function and stability by creating binding sites for m6A reader proteins or by altering the RNA structure within 20–22 nucleotides [15]. YTH domain family proteins, such as YTHDF1, YTHDF2, and YTHDF3, are localized in the cytoplasm and regulate cell survival, proliferation, and migration by promoting RNA degradation [16]. In contrast, YTHDC1, which primarily resides in the nucleus but also shuttles to the cytoplasm, is crucial for mRNA splicing, export, and stability [10]. Despite its significance, the role of YTHDC1 in cell survival and ischemic stroke remains poorly understood. In this study, we identified m6A modification as a primary factor contributing to the accumulation of lncRNA *CRNDE* in both OGD/R-treated neuronal cells and the MCAO rat model. We found that lncRNA *CRNDE*, modified by *METTL3*, influences neural cell functions such as apoptosis and autophagy, mediated through downstream interactions with YTHDF1.

Autophagy is a conserved cellular process responsible for the degradation of damaged cytoplasmic components within lysosomes [17]. It plays a critical role in maintaining cell homeostasis and promoting cell survival under stress conditions [18]. Autophagy is usually initiated with the formation of isolation membranes (or phagophores) that sequester cytoplasmic material. These membranes elongate to form double-membrane autophagosomes [19], which subsequently fuse with lysosomes to form autolysosomes, where the sequestered contents are degraded by lysosomal enzymes [20]. Key ubiquitin-like conjugation systems involved in autophagosome formation include the ATG12-ATG5 system and the MAP1LC3/LC3/Atg8-phosphatidylethanolamine (PE) conjugate. In this process, ATG12 is activated by the E1-like enzyme ATG7, transferred to the E2-like enzyme *ATG10*, and conjugated to ATG5 to form the ATG12-ATG5 conjugate [21]. Bioinformatics analyses have identified an interaction between YTHDC1 and *ATG10*, suggesting that *ATG10* may play a role in neuronal autophagy, warranting further investigation.

To improve cerebral I/R injury, it is essential to explore the relationships among *METTL3*, lncRNA *CRNDE*, m6A modification, YTHDC1, and *ATG10*. The m6A modification of lncRNA *CRNDE*, through its interaction with YTHDC1, may promote the degradation of *ATG10*. Given that *ATG10* is involved in the autophagy process, its degradation could potentially ameliorate cerebral I/R injury. Therefore, investigating

how *METTL3*-mediated m6A modification of lncRNA *CRNDE* promotes *ATG10* degradation through YTHDC1, and its subsequent impact on cerebral I/R injury, could reveal significant insights into this role of mechanism in disease development. Such research may offer new perspectives and targets for developing novel treatment strategies and therapeutic agents.

## Materials and methods

### Middle cerebral artery occlusion (MCAO) modeling

Twenty-four male Sprague-Dawley (SD) rats, aged 8–10 weeks and weighing approximately 250 g, were purchased from Hunan Shengjia Experimental Animal Co., Ltd. After a 7-day adaptation period and overnight fasting, the rats were randomly assigned to one of four groups, with six animals in each group: Sham, MCAO, sh-NC, and sh-lncRNA *CRNDE*. Rats in the Sham group were exposed only to the right middle cerebral artery without suturing. Rats in the MCAO, sh-NC, and sh-lncRNA *CRNDE* group underwent middle cerebral artery occlusion/reperfusion (MCAO/R) surgery [22]. Rats in both sh-NC and sh-lncRNA *CRNDE* groups were injected with Lentiviral particles containing sh-NC or lncRNA CRNDE ($1 \times 10^8$ TU/mL) mixed with saline via the tail vein one week before MCAO/R surgery [23]. Lentiviral particles containing sh-NC and lncRNA CRNDE were designed and synthesized by GenePharma (Shanghai, China). Neurological function was evaluated 3–7 days after MCAO using the Zea Long 5-point scoring system. The scoring was as follows: 0 for no evidence of nerve damage. 1 for inability to fully extend the left front leg. 2 for circling to the left while walking. 3 for unstable posture. And 4 for severe impairment, such as lack of confidence and inability to speak. Neurological testing was conducted by an observer who was blinded to the group assignments. After euthanasia, brain samples were collected and immediately placed into a weighing bottle. The initial wet weight was recorded before the samples were dried. Once the drying process was complete, the final dry weight was measured. The wet-to-dry ratio was then calculated as the ratio of the wet weight to the dry weight. All procedures adhered to ethical standards for animal use and were approved under protocol number 2023-049.

### Cell culture

The SH-SY5Y cells (CM-0208, Pricella, China) were used for the study. First, the SH-SY5Y cells were divided into Control group and OGD/R group. The Control group involved placing the SH-SY5Y cells under conditions of 37℃, 5% $CO_2$, and 95% air. The OGD/R group underwent OGD/R treatment to establish an i*n vitro* ischemic stroke model simulating

MCAO injury. During the hypoxic stage, the cells were treated with Dulbecco's Phosphate-Buffered Saline (DPBS) and placed in a hypoxic environment (37℃, 0% $O_2$, and 5% $CO_2$) for 5 h. During the reoxygenation stage, the DPBS was removed, and the cells were cultured normally in DMEM of 37℃, 5% $CO_2$, and 95% air for 24 h. Next, we silenced lncRNA *CRNDE* and overexpressed *METTL3* in the OGD/R-treated SH-SY5Y cells, dividing them into 4 groups: sh-NC, sh-lncRNA *CRNDE*, sh-lncRNA *CRNDE*+oe-NC, and sh-lncRNA *CRNDE*+oe-*YTHDC1*. sh-NC (SH-SY5Y cells were transfected with sh-NC negative control plasmid and treated with OGD/R), sh-lncRNA *CRNDE* (SH-SY5Y cells were transfected with lncRNA *CRNDE* silencing plasmid and treated with OGD/R), sh-lncRNA *CRNDE*+oe-NC (SH-SY5Y cells were transfected with lncRNA *CRNDE* silencing plasmid and oe-NC negative control plasmid and then treated with OGD/R), sh-lncRNA *CRNDE*+oe-*YTHDC1* (SH-SY5Y cells were transfected with lncRNA *CRNDE* silencing plasmid and *YTHDC1* overexpression plasmid and then treated with OGD/R). To further investigate whether *METTL3* can reverse the effects of lncRNA *CRNDE* on cells, the OGD/R-treated SH-SY5Y cells were divided into 4 groups: oe-NC, oe-*METTL3*, oe-*METTL3*+oe-NC, and oe-*METTL3*+oe-*CRNDE*. oe-NC (SH-SY5Y cells were transfected with oe-NC negative control plasmid and treated with OGD/R), oe-*METTL3* (SH-SY5Y cells were transfected with overexpressing *METTL3* plasmid and treated with OGD/R), oe-*METTL3*+oe-NC (SH-SY5Y cells were transfected with overexpressing *METTL3* plasmid and oe-NC negative control plasmid and then treated with OGD/R), oe-*METTL3*+oe-*CRNDE* (SH-SY5Y cells were transfected overexpressing *METTL3* and *CRNDE* plasmids and then treated with OGD/R). According to the manufacturer's instructions, cells were transfected using Lipofectamine™ 2000 reagent kit (11668500, ThermoFisher, USA). All plasmids were obtained from Abiowell company in Changsha, China [24].

### Morris water maze

The Morris water maze consists of a circular pool with a diameter of 130 cm and a height of 50 cm, filled with water to a depth of 30 cm. The pool is divided into four quadrants (I-IV), and a glass platform with a diameter of 11 cm and a height of 29 cm is placed in the fourth quadrant. The maze is surrounded by blue curtains, and visual cues are positioned around the maze to aid spatial navigation. Cameras connected to a computer system are positioned above the maze to record the rats' trajectories. For the spatial learning test, rats were trained in the water maze for 4 consecutive days. On each day, a quadrant was randomly

selected as the starting point, and rats were placed into the water facing the wall. The time taken for the rats to locate the glass platform (latency) and their swimming trajectories were recorded. If a rat did not find the platform within 60 s, it was guided to the platform using a glass rod, and the latency was recorded as 60 s. After a 30-second rest, the test continued with a different quadrant. On the fifth day, a probe trial was conducted. The glass platform was removed, and the rats were placed in the quadrant where the platform had previously been located. The time spent by the rats in the quadrant where the platform was previously located and the number of crossings over the former platform location were recorded. During all tests, the water temperature was maintained at $23 \pm 3℃$ [25].

### 7 2,3,5-triphenyltetrazolium Chloride (TTC) staining assay
Cerebral infarct volume was assessed using TTC staining (Sigma, MO, USA). At the end of the experiment, the rats were anesthetized and sacrificed, and their brains were immediately removed. The brains were then frozen at-20℃ for 1 min and sectioned into six 2-mm coronal slices. The slices were stained with 2% TTC solution at 37℃ for 30 min, followed by the removal of TTC and fixation in 4% paraformaldehyde for 24 h. Normal brain tissue stained red, while infarcted tissue remained unstained (white). The infarct volume was quantified using AlphaEase software (Alpha Innotech, San Leandro, CA).

### Hematoxylin-eosin (HE) staining
The slides were first rinsed with distilled water for 5 min, counterstained with hematoxylin (AWI0009a, Abiowell, China) for 1 to 10 min, and then rinsed again with distilled water. The slides were subsequently stained blue with PBS (AWC0217, Abiowell, China) at pH 7.4. Eosin (AWI0029a, Abiowell, China) was applied for 1 to 5 min, followed by another rinse with distilled water. The slides were then dehydrated in graded alcohol (95–100%) for 5 min or dried directly.

### Terminal deoxynucleotidyl transferase dUTP nick end labeling (TUNEL)
The Proteinase K (39450-01-6, aladdin, China) working solution was prepared by diluting 1 μL of 100× Proteinase K in 99 μL of 1× PBS per sample. After removing excess 1× Equilibration Buffer with absorbent paper, 50 μL of TdT incubation buffer was added to the sample tissue. Incubation occurred at 37℃ for 60 s, protected from drying and light. The samples were rinsed three times with PBS for 5 s each. The nuclei were stained with a DAPI (AWC0292, Abiowell, China) working solution at 37℃ for 10 min, followed by three 5-second rinses with PBS, avoiding light exposure.

### Transmission electron microscopy (TEM)
The fixed tissues were transferred into PBS buffer and incubated for 6 h. Dehydration was performed sequentially in 80% ethanol for 10 s, 95% ethanol for 15 s, and twice in 100% ethanol for 50 s each. The tissues were then immersed in epoxy propane (M25514, Meryer, China) for 30 s. After embedding in pure epoxy resin, the samples were baked in a 40℃ oven for 12 h and then at 60℃ for 48 h. The embedded blocks were trimmed, and ultrathin sections were cut and placed onto copper grids. The sections were stained with lead and uranium and examined using a TEM (JEM1400, JEOL, Japan). Images were captured with a Morada G3 digital camera.

### Quantitative real-time polymerase chain reaction (qRT-PCR)
Total RNA was extracted from cells using the TRIzol method. cDNA was synthesized from RNA samples using a Reverse Transcription kit. Quantitative PCR amplification was performed with UltraSYBR Mixture (CW2601, CWBIO, China) and a fluorescence quantitative PCR instrument (QuantStudio1, ABI). Gene expression levels were determined using the $2^{-\Delta\Delta Ct}$ method, with GAPDH as the reference gene. The sequences of the primers are provided in Table 1.

### Western blot
Total protein was extracted from cells and tissues using the RIPA Kit (r0010, Solarbio, China). The proteins were separated by SDS-PAGE and transferred to PVDF membranes. Primary antibodies used included rabbit anti-ATG10 (1:5000 dilution, ab124711, Abcam), rabbit anti-LC3 (1:3000 dilution, 14600-1-AP, Proteintech), rabbit anti-Beclin1 (1:2000 dilution, 11306-1-AP, Proteintech), mouse anti-p62 (1:10000 dilution, 66184-1-Ig, Proteintech), rabbit anti-Bax (1:5000 dilution, 60178-1-Ig, Proteintech), rabbit anti-Caspase-3 (1:1000 dilution, #9664, CST), mouse anti-Bcl-2 (1:5000 dilution, ab13867, Abcam), rabbit anti-METTL3 (1:1000 dilution, ab195352, Abcam), and rabbit anti-YTHDC1 (1:1000 dilution, ab259990, Abcam). Following incubation with primary antibodies, the membranes were rinsed three times for 10 s each with Tris-buffered saline-Tween (TBST). ECL chemiluminescent solution (K-12045-D50, Advansta) was applied for 1 min, and images of the target bands were captured using a chemiluminescent imaging system (ChemiScope 6100, Qinxiang, China). GAPDH served as the internal reference. ImageJ software (National Institutes of Health, USA) was used to

Yu *et al. Biology Direct*    (2024) 19:92

Page 5 of 17

**Table 1** Primer sequences

| Gene | Sequences (5'-3') |
|------|-------------------|
| R-lncRNA *CRNDE* | F: GGCTTCCCGAGATGTGTTTG |
| | R: TGGGGAACACTCTAGTCCACA |
| R-*ATG10* | F: GCGAGCGGGTTCCCATT |
| | R: TTCTCCATTCCCAGCCATCG |
| R-*LC3* | F: AACACAGCCACCTCTCGACCT |
| | R: ACACAACCCACACACGGCAG |
| R-*Beclin1* | F: GTGGCGGCTCCTATTCCATC |
| | R: GACACCCAAGCAAGACCCCA |
| R-*p62* | F: AGCATACAGAGAGCACCCAT |
| | R: ACATACAGAAGCCAGAATGCAG |
| R-*GAPDH* | F: ACAGCAACAGGGTGGTGGAC |
| | R: TTTGAGGGTGCAGCGAACTT |
| H-lncRNA *CRNDE* | F: ATTCATCCCAAGGCTGGTCTG |
| | R: CTCCTCCTTCCAATAGCCAGT |
| H-*ATG10* | F: CACGGCCACTTCTGGTTGG |
| | R: GGTGACCCTACGGAACTGAAT |
| H-*LC3* | F: CTTCAGGTTCACAAAACCCGC |
| | R: GGTTGCGCTTCACAACTCAG |
| H-*Beclin1* | F: GGGCTCCCGAGGGATGG |
| | R: AGTTCCTGGATGGTGACACG |
| H-*p62* | F: TGAGTGCCGCGTACCA |
| | R: CCATGTTGCACGCCAAAC |
| H-*METTL3* | F: ATATTCACATGGAACTGCCCTA |
| | R: ATTTCATCTACCCGTTCATACCC |
| H-*GAPDH* | F: ACAGCCTCAAGATCATCAGC |
| | R: GGTCATGAGTCCTTCCACGAT |

analyze the gray values of the target bands. The relative expression of each target protein was calculated as the gray value of the target protein divided by the gray value of the internal reference protein. Full-length Western blot bands are shown in Figure S1.

### Flow cytometry
The cells were digested with trypsin without EDTA, collected, and washed twice with PBS. After centrifugation at 2000 rpm for 5 min, approximately $5 \times 10^5$ cells were suspended in 500 µL of binding buffer (A377916, Aladdin, China). To the suspension, 5 µL of Annexin V-FITC (KGA108, KeyGen, China) and 5 µL of propidium iodide (PI) were added. The mixture was incubated at room temperature, protected from light, for 15 min. Flow cytometry (A00-1-1102. Beckman, USA) was used for detection and analysis.

### Enzyme-linked immunosorbent assay (ELISA)
ELISA kits for TNF-α (CSB-E04740h), IL-1β (CSB-E08053h), IL-6 (CSB-E04638h), and IL-10 (CSB-E04593h) were obtained from Wuhan Huamei Biotechnology Co., Ltd. Reagents were prepared according to the manufacturer's instructions. Samples were added to the designated wells of the ELISA plate, which included standard and test sample wells. After

discarding the liquid and tapping the plate dry without washing, each well was washed with 200 µL of wash buffer for 2 min and tapped dry. Within 5 min of terminating the reaction, the optical density (OD) was measured at 450 nm using a microplate reader (MB-530, HEALES, China).

### RNA binding protein immunoprecipitation-realtime fluorescence quantitative PCR (RIP-qPCR)
Two centrifuge tubes were prepared for each sample and labeled as IP and Normal IgG (30000-0-AP, Proteintech) respectively. The collected supernatant was added to a tube containing 900 µL of RIP immunoprecipitation buffer and inverted overnight at 4℃. To prepare the input tube, take 10 µL of lysis buffer, mix it with 2x SDS loading buffer, and incubate at 95 ℃ for 5 min. Remove the tube from the magnetic field, add 500 µL of RIP Wash Buffer, and shake gently. Finally, add 250 µL of RIP Wash Buffer to each tube. The reverse transcription product can be directly used for PCR and fluorescence quantitative PCR reactions.

### Methylated RNA immunoprecipitation (MeRIP)
The plate was gently tilted or shaken from one side to the other several times to mix the solution. Ensure that the solution is evenly covering the bottom of the well. For single point controls, 2 µL of positive control at a concentration of 0.5 ng/µL was added. The final concentrations were 0.02, 0.2, 0.1, 0.4, and 1 ng/well, respectively. To achieve optimal binding, the amount of RNA sample added should not exceed 8 µL. The samples should be monitored closely to control color changes effectively. Blocking solution (100 µL) was added to each well to block the enzyme reaction. After adding the stop solution, the color turned yellow, and the absorbance was read at 450 nm within 2 to 10 min.

### Statistical analyses
All measurement data are expressed as mean ± standard deviation (SD). Data analysis was conducted using SPSS 26.0 software (IBM, Armonk, NY, USA). An unpaired Student's t-test was employed to compare data between two groups that were not one-to-one correspondences. One-way ANOVA followed by Tukey's post-hoc test was used for comparisons among multiple groups. Pearson correlation analysis was used to assess the relationship between two variables. A $p$-value less than 0.05 was considered statistically significant.

Yu *et al. Biology Direct*        (2024) 19:92

Page 6 of 17

## Results

### lncRNA *CRNDE* is highly expressed in MCAO rats and correlates with autophagy

The MCAO rat model was constructed, and pathological changes were assessed. The results showed that compared to the sham-operated group, rats in the MCAO group exhibited reduced swimming speed, increased latency, and extended time to cross the platform (Fig. 1A, B). Infarct size and water content in the MCAO group were significantly greater than those in the sham-operated group (Fig. 1C, D). Pathological examination revealed well-preserved cortical structure in the Sham group with no intercellular edema, organized cell arrangement, and consistent staining. In contrast, the MCAO group exhibited liquefactive necrosis, disorganized cell arrangement, edema around the injury site, cell nucleus shrinkage or dissolution, and inflammatory cell infiltration (Fig. 1E). Apoptotic cells were elevated in the MCAO group (Fig. 1F). lncRNA *CRNDE* expression was significantly higher in the MCAO group compared to the Sham group and also increased in hypoxia-damaged SH-SY5Y cells relative to undamaged cells (Fig. 1G). The mRNA expression of *ATG10*, *LC3*, and *Beclin1* was elevated, while the expression of *p62* was reduced in the MCAO group (Fig. 1H). Furthermore, the protein expression of ATG10, LC3II/I, and Beclin1 was increased, whereas the expression of p62 was diminished in the MCAO group, suggesting the induction of autophagy (Fig. 1I). Correlation analysis revealed that lncRNA *CRNDE* positively correlated with *ATG10*, *LC3*, and *Beclin1* and negatively correlated with *p62* (Fig. 1J). These results suggested aberrant expression of lncRNA *CRNDE* and autophagy-related genes in MCAO rats.

### Silencing lncRNA *CRNDE* inhibits OGD/R-induced SH-SY5Y cell apoptosis and inflammation and promotes autophagy

We constructed an OGD/R model in SH-SY5Y cells and silenced lncRNA *CRNDE* to assess its impact on cell phenotype. The OGD/R group exhibited increased lncRNA *CRNDE* expression, while the sh-lncRNA *CRNDE* group showed decreased expression, confirming effective silencing (Fig. 2A). In the OGD/R group, cell apoptosis was elevated, evidenced by increased Bax and Caspase-3 levels and decreased Bcl-2 expression. In contrast, the sh-lncRNA *CRNDE* group demonstrated reduced apoptosis, with lower Bax and Caspase-3 levels and higher Bcl-2 expression (Fig. 2B and C). Inflammatory factor levels were higher in the OGD/R group, with increased TNF-α, IL-1β, and IL-6, and decreased IL-10. The sh-lncRNA *CRNDE* group had lower TNF-α, IL-1β, and IL-6 levels, and higher IL-10 (Fig. 2D). In the context of autophagy, the

OGD/R group demonstrated increased mRNA expression of *ATG10*, *Beclin1*, and *LC3*, while *p62* expression decreased. Conversely, the sh-lncRNA *CRNDE* group displayed reduced levels of ATG10, Beclin1, and LC3, with increased p62 expression (Fig. 2E). Additionally, the OGD/R group exhibited increased protein expression of ATG10, Beclin1, and LC3II/I, along with decreased p62 expression. In contrast, the sh-lncRNA *CRNDE* group showed reduced levels of ATG10, Beclin1, and LC3II/I, while p62 expression increased (Fig. 2F). In summary, silencing lncRNA *CRNDE* reduces apoptosis and inflammation and affects autophagy in OGD/R-induced SH-SY5Y cells.

### Silencing lncRNA *CRNDE* could alleviate I/R Injury

The above results from the SH-SY5Y cell model indicated that silencing lncRNA *CRNDE* reduced apoptosis and enhanced autophagy. To validate these findings in an animal model, we examined the effects of silencing lncRNA *CRNDE* in a rat MCAO model. As shown in Fig. 3A, mice treated with sh-lncRNA *CRNDE* exhibited improved behavioral outcomes, including faster swimming speed, shorter latency, and reduced time spent on the platform, compared to the sh-NC group (Fig. 3B). Post-mortem analysis revealed a significant reduction in infarct size and water content in the brains of the sh-lncRNA *CRNDE* group compared to the sh-NC group (Fig. 3C and D). Pathological examination of brain tissues further supported these observations. The sh-NC group exhibited extensive necrosis and inflammatory cell infiltration in the ischemic cortical tissue, whereas the sh-lncRNA *CRNDE* group showed reduced necrosis and inflammatory infiltration (Fig. 3E), along with fewer apoptotic cells (Fig. 3F). Quantitative analysis confirmed that lncRNA *CRNDE* expression was significantly lower in the sh-lncRNA *CRNDE* group compared to the sh-NC group (Fig. 3G). In addition, the sh-lncRNA *CRNDE* group showed increased mRNA expression of autophagy-related genes *ATG10*, *LC3*, and *Beclin1*, and decreased expression of *p62* (Fig. 3H). Furthermore, the sh-lncRNA *CRNDE* group showed increased protein expression of autophagy-related genes ATG10, LC3II/I, and Beclin1, and decreased expression of p62 (Fig. 3I). Electron microscopy revealed that in the sh-NC group, cellular proteins and organelles were transported to lysosomes for degradation. In contrast, the sh-lncRNA *CRNDE* group showed more extensive dissolution of organelles, indicating enhanced autophagy (Fig. 3J). Taken together, silencing lncRNA *CRNDE* alleviates brain tissue damage and promotes autophagy, as demonstrated by improved behavioral outcomes, reduced infarct size, and enhanced autophagic activity in the MCAO rat model.
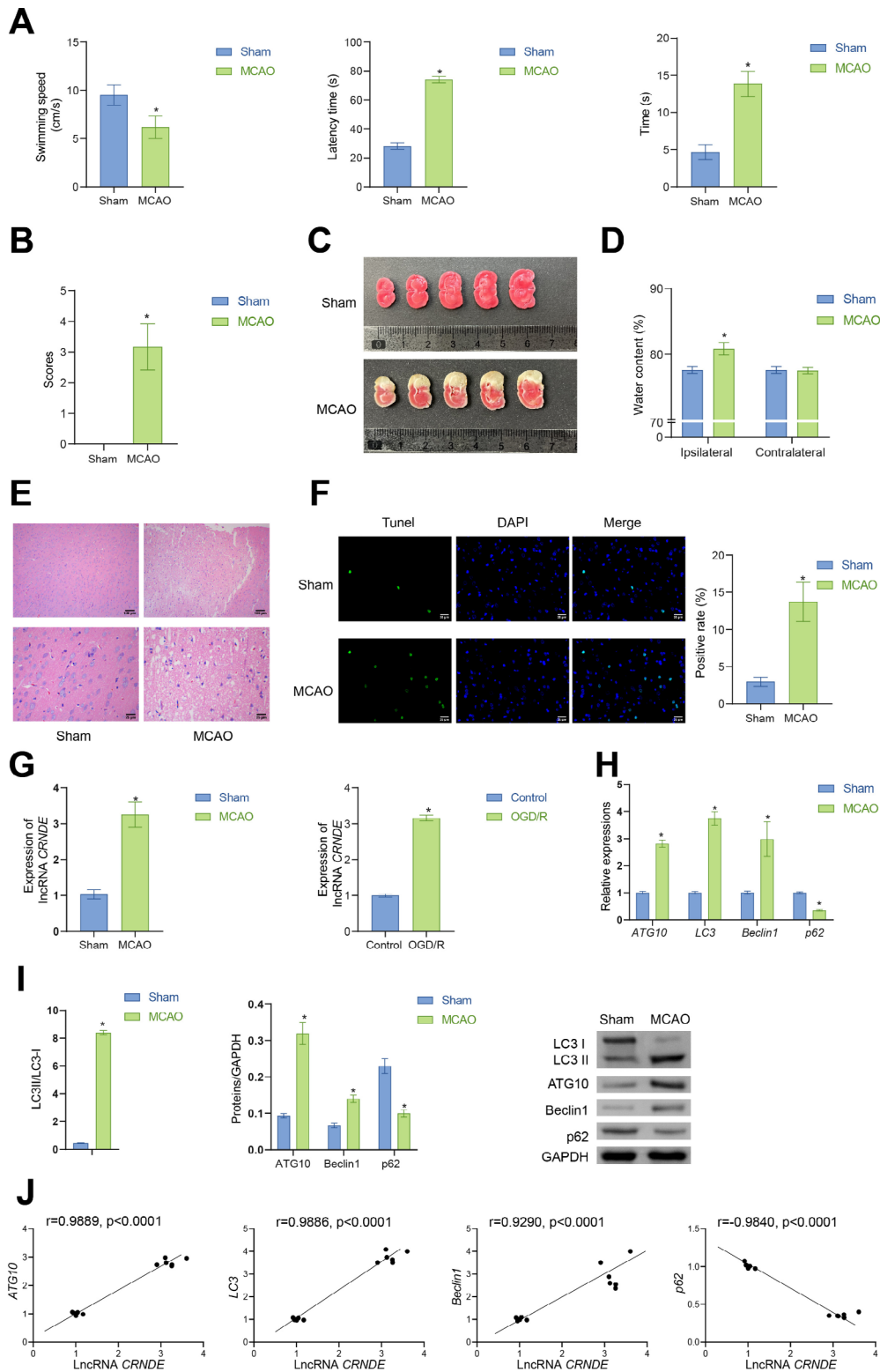
**Fig. 1** Elevated lncRNA *CRNDE* levels in MCAO rats. (**A**) Behavioral assessment using the Morris water maze. (**B**) Neurological function score. (**C**) TTC staining for brain infarction evaluation. (**D**) Assessment of brain water content. (**E**) HE staining for observation of MCAO-induced injury. (**F**) TUNEL assay to detect cell apoptosis. (**G**) Measurement of lncRNA *CRNDE* expression levels. (**H**) qRT-PCR analysis of *ATG10*, *LC3*, *Beclin1, and* p62 mRNA. (**I**) Western blot analysis of ATG10, LC3II/I, Beclin1, and p62 protein levels. (**J**) Correlation analysis between lncRNA *CRNDE* and *ATG10*, *LC3*, *Beclin1, and p62*. *$P < 0.05$ indicates a significant difference compared to the Sham group. Data are expressed as Mean ± SD. Comparisons between two groups were performed using the unpaired Student's t-test, and Pearson correlation was used for correlation analysis
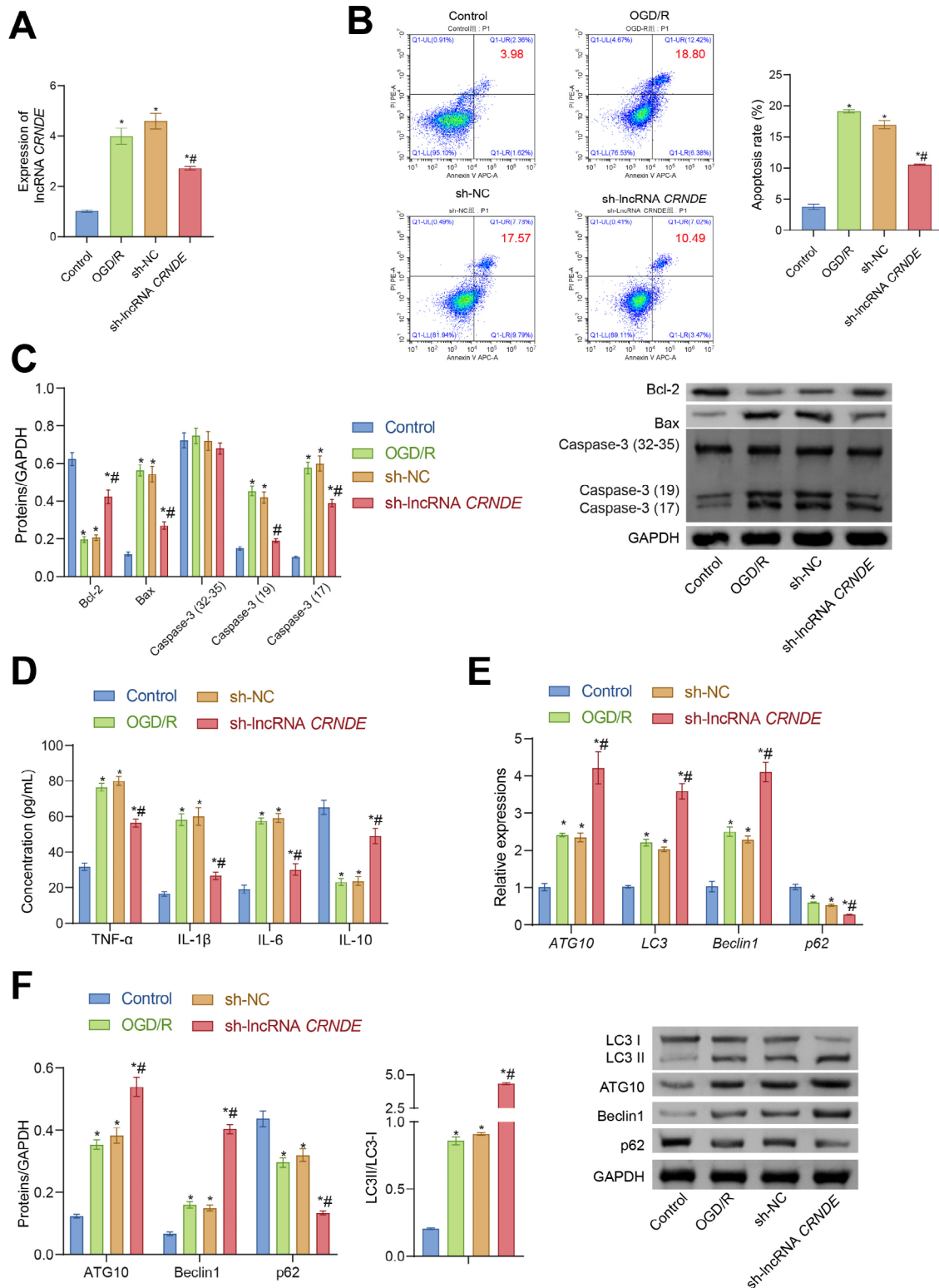
**Fig. 2** Effect of silencing lncRNA *CRNDE* on apoptosis and autophagy in OGD/R-induced SH-SY5Y cells. (**A**) Expression levels of lncRNA *CRNDE* in cells. (**B**) Flow cytometry analysis of apoptosis rate. (**C**) Protein expression of Bcl-2, Bax, and Caspase-3. (**D**) Measurement of inflammatory factor levels. (**E**) Expression of autophagy-related markers *ATG10*, *LC3*, *Beclin1*, and *p62*. (**F**) Quantification of ATG10, LC3II/I, Beclin1, and p62 protein levels. *$P < 0.05$ indicates a significant difference compared to the Control group. #$P < 0.05$ indicates a significant difference compared to the sh-NC group. Data are presented as Mean $\pm$ SD. One-way ANOVA followed by Tukey's post-hoc test was used for comparisons among multiple groups
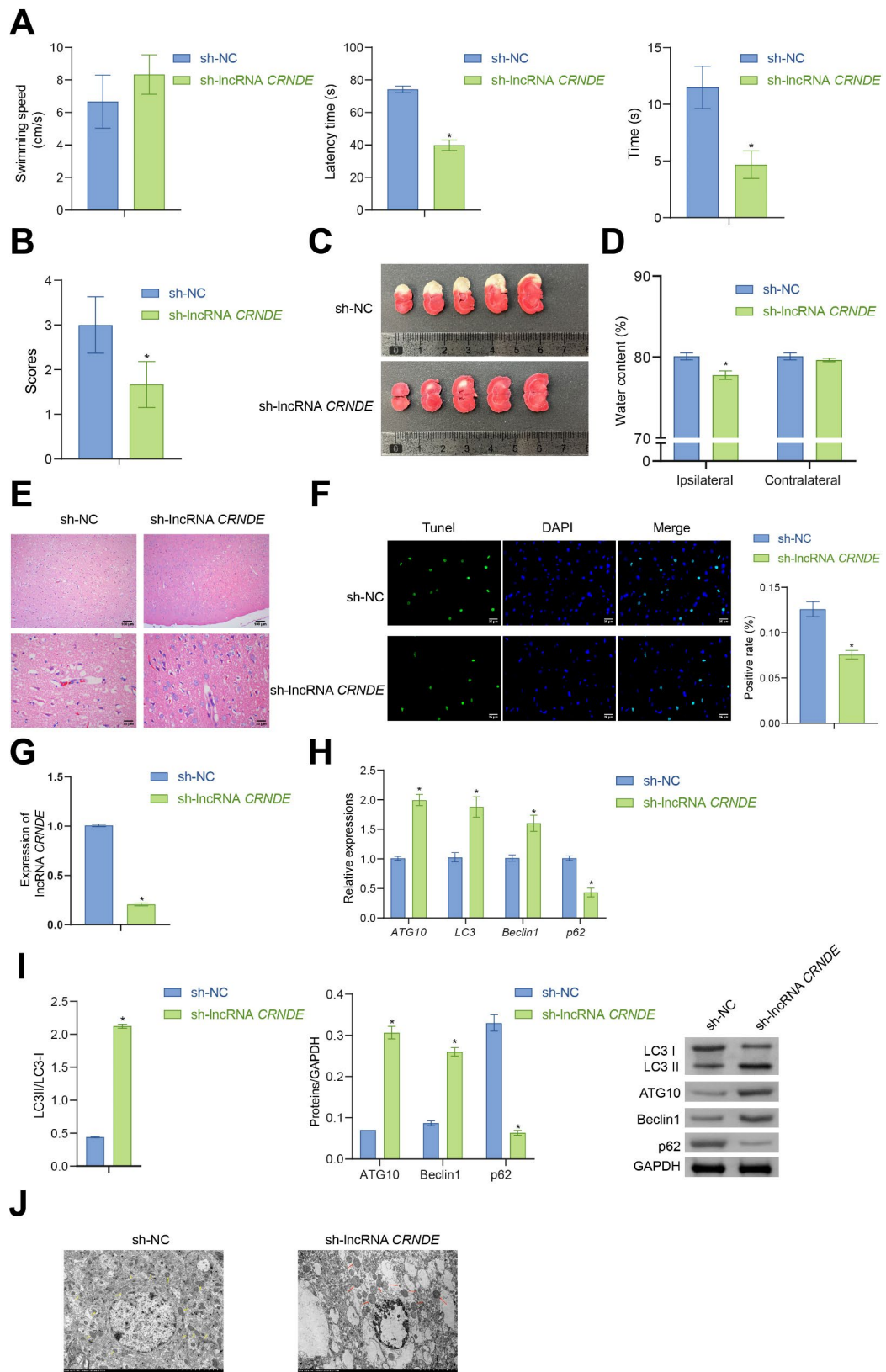
**Fig. 3** (See legend on next page.)

(See figure on previous page.)

**Fig. 3** Inhibiting lncRNA *CRNDE* suppresses further damage to brain tissues and promotes autophagy. (**A**) Rat swimming speed, latency time, and time spent on the platform in the Morris water maze. (**B**) Neurological function score. (**C**) TTC staining for evaluation of cerebral infarction area. (**D**) Assessment of brain water content. (**E**) HE staining for visualization of MCAO-induced injury. (**F**) TUNEL assay for detecting apoptosis. (**G**) Expression levels of lncRNA *CRNDE* in brain injury tissues. (**H**) mRNA levels of autophagy-related markers *ATG10, LC3, Beclin1, and p62*. (**I**) Protein levels of autophagy-related markers ATG10, LC3II/I, Beclin1, and p62. (**J**) Autophagy in brain tissues (red and yellow arrows indicate pyroptotic bodies). *$P < 0.05$ indicates a significant difference compared to the sh-NC group. Data are expressed as Mean±SD. Comparisons between two groups were performed using the unpaired Student's t-test

## lncRNA *CRNDE* and YTHDC1 inhibit OGD/R-induced apoptosis, inflammation and enhance autophagy in SH-SY5Y cells

Silencing lncRNA *CRNDE* was shown to inhibit brain tissue damage and promote autophagy. To further explore the regulatory mechanisms of lncRNA *CRNDE*, we investigated its interaction with the m6A-related gene *YTHDC1*. Bioinformatics analysis identified a potential interaction between lncRNA *CRNDE* and YTHDC1, which was subsequently confirmed through RNA pull-down and protein immunoblotting (Fig. 4A). RNA immunoprecipitation (RIP) experiments demonstrated that lncRNA *CRNDE* was enriched in YTHDC1-bound fractions (Fig. 4B). Although there was no significant difference in YTHDC1 expression between the sh-NC and sh-lncRNA *CRNDE* groups (Fig. 4C), In the oe-*YTHDC1* group led to increased YTHDC1 levels compared to the oe-NC group (Fig. 4D). In SH-SY5Y cells, silencing lncRNA *CRNDE* resulted in decreased apoptosis, reduced Bax and Caspase-3 expression, and increased Bcl-2 expression compared to the sh-NC group (Fig. 4E and F). In sh-lncRNA *CRNDE*+oe-*YTHDC1* group, cell apoptosis increased, along with elevated Bax and Caspase-3 levels and decreased Bcl-2 levels. This suggested that overexpression of YTHDC1 can reverse the anti-apoptotic effects of lncRNA *CRNDE* silencing. Analysis of inflammatory cytokines showed that the sh-lncRNA *CRNDE* group had lower levels of TNF-α, IL-1β, and IL-6, and higher levels of IL-10 compared to the sh-NC group. In contrast, the sh-lncRNA *CRNDE*+oe-*YTHDC1* group had increased levels of TNF-α, IL-1β, and IL-6, and decreased levels of IL-10, indicating that *YTHDC1* overexpression promotes inflammatory cytokine secretion (Fig. 4G). Autophagy-related analysis revealed that compared to the sh-NC group, silencing lncRNA *CRNDE* increased the mRNA expression of *LC3* and *Beclin1*, and decreased *p62* expression. On the contrary, in the sh-lncRNA *CRNDE*+oe-*YTHDC1* group, the expression of *LC3* and *Beclin1* decreased, while *p62* expression increased (Fig. 4H). Furthermore, compared to the sh-NC group, silencing lncRNA *CRNDE* increased the protein expression of LC3II/I and Beclin1, and decreased p62 expression. Conversely, in the sh-lncRNA *CRNDE*+oe-*YTHDC1* group, the expression of LC3II/I and Beclin1 decreased, while p62 expression increased (Fig. 4I).

These results suggested that YTHDC1 could modulate autophagy by counteracting the effects of lncRNA *CRNDE* silencing.

## lncRNA *CRNDE* interacts with YTHDC1 to promote *ATG10* expression

To determine if the interaction between lncRNA *CRNDE* and YTHDC1 affects *ATG10* expression, RIP experiments assessed *ATG10* enrichment following lncRNA *CRNDE* overexpression. The sh-lncRNA *CRNDE* group showed a substantial reduction in *ATG10* enrichment compared to the oe-NC group (Fig. 5A), indicating that lncRNA *CRNDE* affects *ATG10* expression. In addition, compared to the sh-NC group, the sh-lncRNA *CRNDE* group showed higher levels of *ATG10* mRNA and ATG10 protein. However, in the sh-lncRNA *CRNDE*+oe-*YTHDC1* group, the mRNA levels of *ATG10* decreased compared to the sh-lncRNA *CRNDE*+oe-NC group, and the ATG10 protein levels also decreased (Fig. 5B and C). To further validate these results, we measured *ATG10* expression in SH-SY5Y cells treated with actinomycin D. Over time, *ATG10* expression decreased, with levels in the sh-lncRNA *CRNDE*+oe-*YTHDC1* group approaching those of the Sham group (Fig. 5D). Overall, both lncRNA *CRNDE* and YTHDC1 regulate *ATG10* expression, with lncRNA *CRNDE* promoting its expression and YTHDC1 exerting an inhibitory effect when overexpressed.

## METTL3 mediates lncRNA *CRNDE* m6A modification to inhibit OGD/R-induced neuronal cell apoptosis and inflammation and promote autophagy

To investigate the role of METTL3 in this process, we assessed m6A modification levels in both Sham and MCAO groups. We observed m6A modifications in both groups, although levels were notably lower in the MCAO group. Within the OGD/R group, m6A levels were reduced compared to the Control group (Fig. 6A). Similarly, the m6A modification of lncRNA *CRNDE* was diminished in the MCAO group and further reduced in the OGD/R group compared to the Control group (Fig. 6B). In vivo and in vitro RNA immunoprecipitation (RIP) experiments revealed decreased METTL3 expression in the model group (Fig. 6C). Overexpression of *METTL3* led to a significant increase in the m6A modification of

lncRNA *CRNDE* (Fig. 6D). Consequently, we generated overexpression models for *METTL3* and *CRNDE* to observe their effects on SH-SY5Y cells. In the oe-*METTL3* group, *METTL3* expression increased, and lncRNA *CRNDE* expression decreased. In the oe-*METTL3*+oe-*CRNDE* group, while *METTL3* levels remained unchanged, lncRNA *CRNDE* expression increased, confirming successful overexpression of both *METTL3* and *CRNDE* (Fig. 6E). In the oe-*METTL3* group, SH-SY5Y cell apoptosis was reduced, with decreased expression of Bax and Caspase-3 and increased expression of Bcl-2. In contrast, in the oe-*METTL3*+oe-*CRNDE* group, apoptosis rates, Bax and Caspase-3 levels, and Bcl-2 expression were elevated compared to the oe-*METTL3*+oe-NC group, indicating that overexpression of *METTL3* can inhibit apoptosis in SH-SY5Y cells (Fig. 6F and G). Inflammatory factor analysis showed that the oe-*METTL3* group had lower levels of TNF-α, IL-1β, and IL-6, and higher levels of IL-10 compared to the oe-NC group. Conversely, the oe-*METTL3*+oe-*CRNDE* group exhibited higher levels of TNF-α, IL-1β, and IL-6, and lower levels of IL-10 compared to the oe-*METTL3*+oe-NC group, suggesting that *METTL3* overexpression suppresses inflammatory cytokine secretion (Fig. 6H). In terms of autophagy, compared to the oe-*METTL3* group, the oe-NC group showed increased mRNA expression of *ATG10*, *LC3*, and *Beclin1*, while *p62* expression decreased. However, in the oe-*METTL3*+oe-*CRNDE* group, compared to the oe-*METTL3*+oe-NC group, levels of *ATG10*, *LC3*, and *Beclin1* decreased, while *p62* levels increased (Fig. 6I). Furthermore, in the oe-*METTL3* group compared to the oe-NC group, protein expression of ATG10, LC3II/I, and Beclin1 increased, while p62 expression decreased. However, in the oe-*METTL3*+oe-*CRNDE* group, compared to the oe-*METTL3*+oe-NC group, levels of ATG10, LC3II/I, and Beclin1 decreased, while p62 levels increased (Fig. 6J). In summary, *METTL3* overexpression mediates the m6A modification of lncRNA *CRNDE*, which inhibits SH-SY5Y cell apoptosis and promotes autophagy.

## Discussion

This study elucidates the critical roles of *METTL3* and lncRNA *CRNDE* in ischemia/reperfusion (I/R) injury. Our findings reveal that lncRNA *CRNDE* interacts with YTHDC1 to modulate the expression of *ATG10*. Specifically, we observed increased m6A modification levels in neurons subjected to OGD/R and in rats treated with MCAO, indicating that *METTL3*, a key methyltransferase, is primarily responsible for the abnormal m6A modification observed. Our data demonstrate that *METTL3* can modify lncRNA *CRNDE*, resulting in decreased expression of this long

non-coding RNA. Silencing lncRNA *CRNDE* reduced apoptosis in SH-SY5Y cells, lowered the levels of pro-inflammatory cytokines TNF-α, IL-1β, and IL-6, increased IL-10 secretion, and promoted autophagy.

LncRNAs regulate various biological processes [26]. Among these, lncRNA *CRNDE* has been identified as an oncogene and is highly expressed in hypoxic-ischemic brain injury. Silencing of lncRNA *CRNDE* has been shown to partially alleviate such injury by promoting autophagy [27]. Additionally, studies have demonstrated that lncRNA *CRNDE* expression is significantly upregulated in retinal cells following ischemia-reperfusion (I/R) and under conditions of high oxygen stress [28]. Our results are consistent with these findings, as we observed higher expression levels of lncRNA *CRNDE* in both the MCAO rat model and OGD/R-treated neurons compared to the sham group. Furthermore, silencing lncRNA *CRNDE* in OGD/R-treated neurons led to a reduction in pro-inflammatory cytokines TNF-α, IL-1β, and IL-6, an increase in IL-10 secretion, decreased apoptosis, and enhanced autophagy.

Studies have demonstrated that m6A expression is significantly higher in the brain compared to other tissues, highlighting the tissue-specific nature of m6A expression in the brain [29]. *METTL3*, a crucial catalytic enzyme, is involved in m6A methylation [30]. Moreover, the induction of YTHDC1 following ischemia aligns with previous observations of altered levels of *YTHDF1* and *YTHDF2* after a stroke [10]. Our findings corroborate these reports, indicating that m6A methylation plays a role in sorting genes into stress granules [31]. In our study, lower m6A levels were observed in both the MCAO rat model and OGD/R-treated SH-SY5Y cells. Overexpression of *METTL3* was found to inhibit lncRNA *CRNDE* expression, leading to reduced apoptosis, decreased pro-inflammatory cytokines TNF-α, IL-1β, and IL-6, increased IL-10 secretion, and enhanced autophagy in SH-SY5Y cells. Conversely, lncRNA *CRNDE* was found to bind to YTHDC1, and overexpression of *YTHDC1* resulted in increased apoptosis, elevated levels of TNF-α, IL-1β, and IL-6, decreased IL-10 secretion, reduced *LC3* and Beclin1 expression, and inhibited autophagy in SH-SY5Y cells.

Recent evidence indicates that modulating autophagic activity can improve the efficacy of various anti-cancer drugs, including oxaliplatin [32], cisplatin [33], doxorubicin [34], and 5-Fu [35]. High expression levels of *ATG10* have been observed in malignant tumors such as colorectal cancer (CRC) [36] and lung cancer [37]. Increased *ATG10* expression is positively correlated with lymphatic invasion and is a predictor of shorter overall survival [37]. Further research has
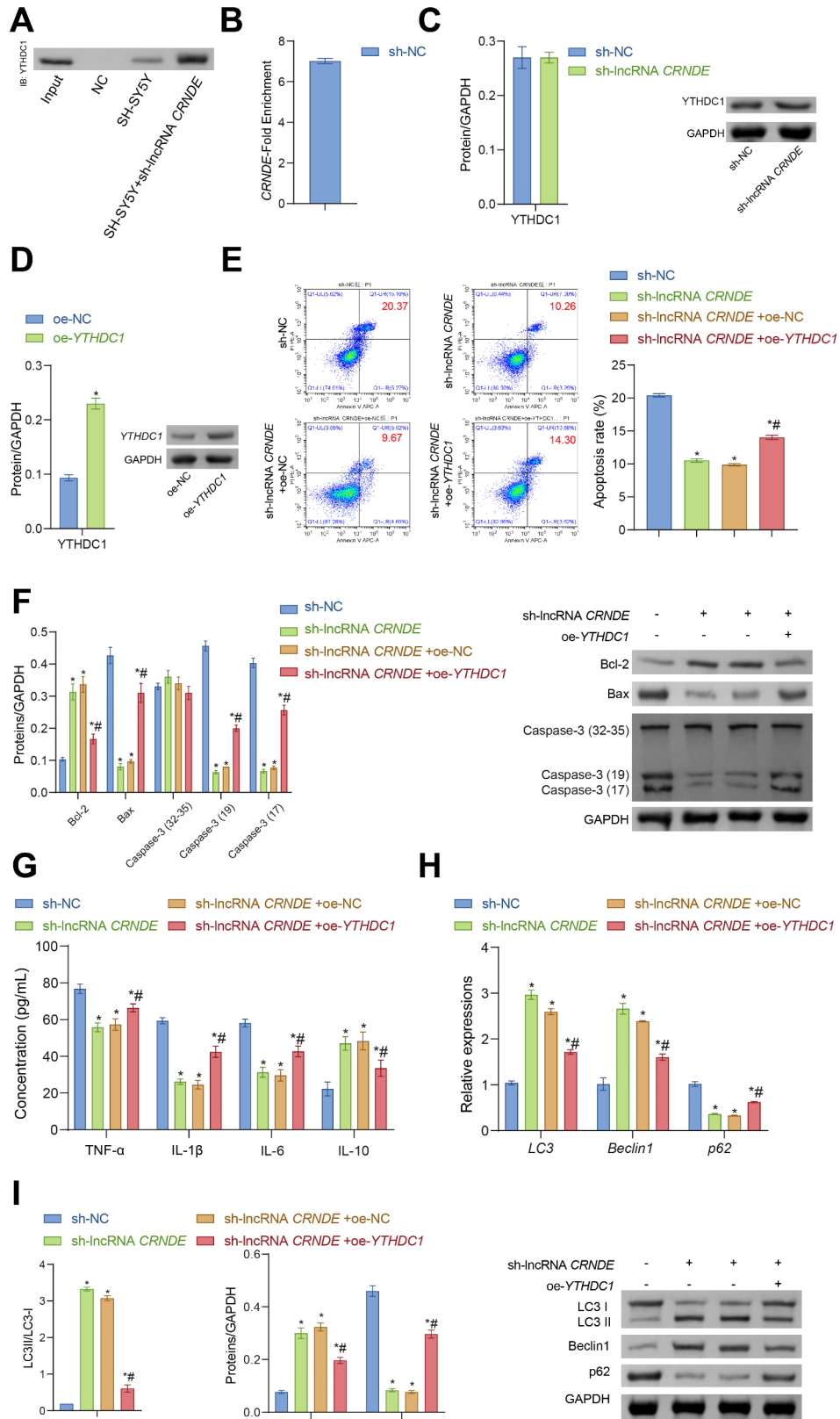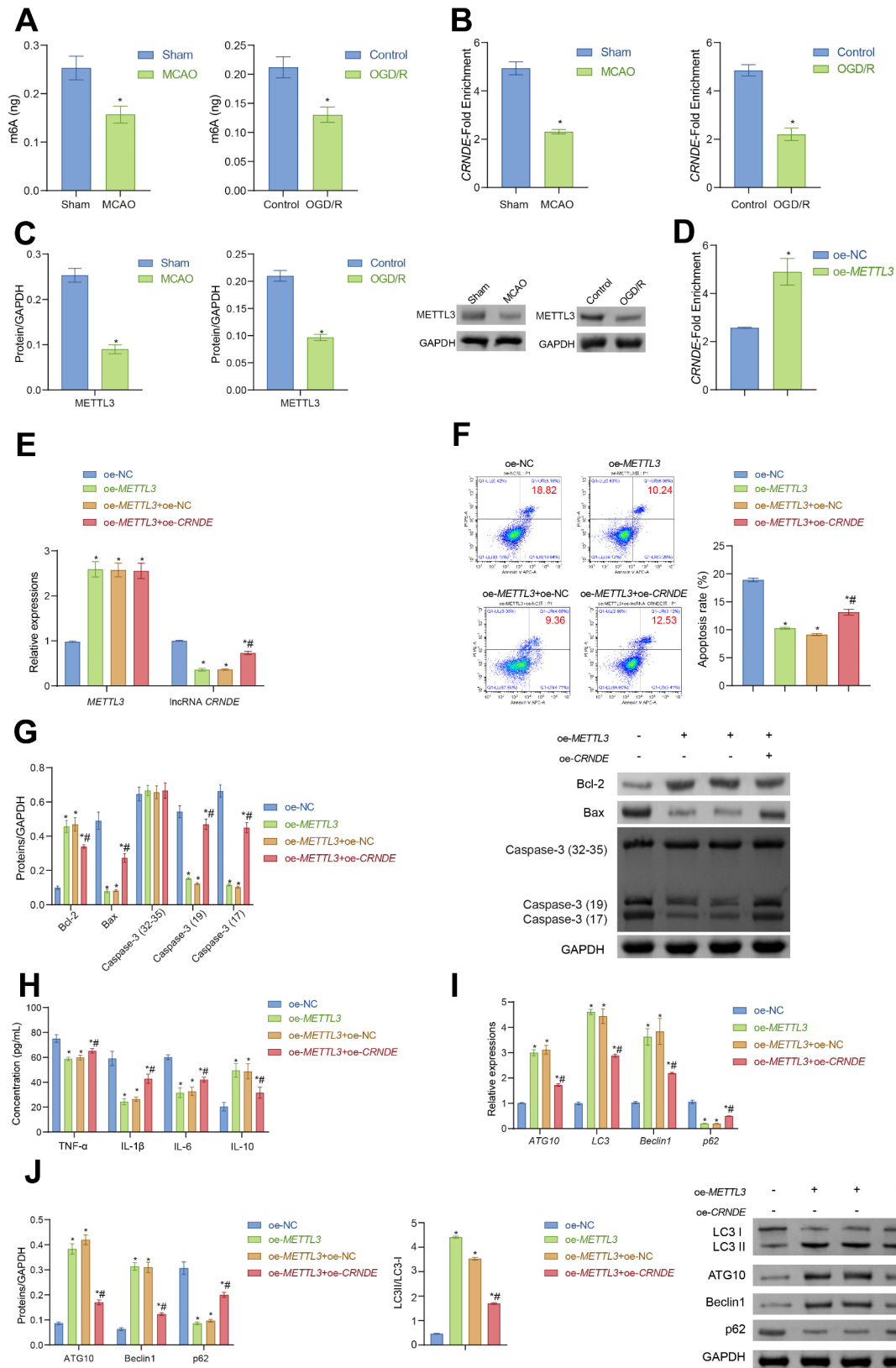
**Fig. 4** (See legend on next page.)

(See figure on previous page.)

**Fig. 4** Interaction of lncRNA *CRNDE* with YTHDC1 inhibits apoptosis in SH-SY5Y cells. (**A**) Pull-down experiment to detect the interaction between ln-cRNA *CRNDE* and YTHDC1. (**B**) RIP assay to measure the expression of lncRNA *CRNDE*. (**C**, **D**) Western blot analysis of YTHDC1 protein expression. (**E**) Flow cytometry analysis of apoptosis rate. (**F**) Western blot analysis of Bcl-2, Bax, and Caspase-3 proteins. (**G**) Levels of inflammatory factors TNF-α, IL-1β, IL-6, and IL-10. (**H**) qRT-PCR analysis of mRNA levels for autophagy-related markers *LC3*, *Beclin1, and p62*. (**I**) Western blot analysis of autophagy-related proteins LC3II/I, Beclin1, and p62. *$P < 0.05$ indicates a significant difference compared to the sh-NC group. #$P < 0.05$ indicates a significant difference compared to the sh-lncRNA *CRNDE* + oe-NC group. All data are expressed as Mean ± SD. Comparisons between two groups were performed using the unpaired Student's t-test, while one-way ANOVA and Tukey's post-hoc test were used for comparisons among multiple groups. All the experiments were repeated thrice
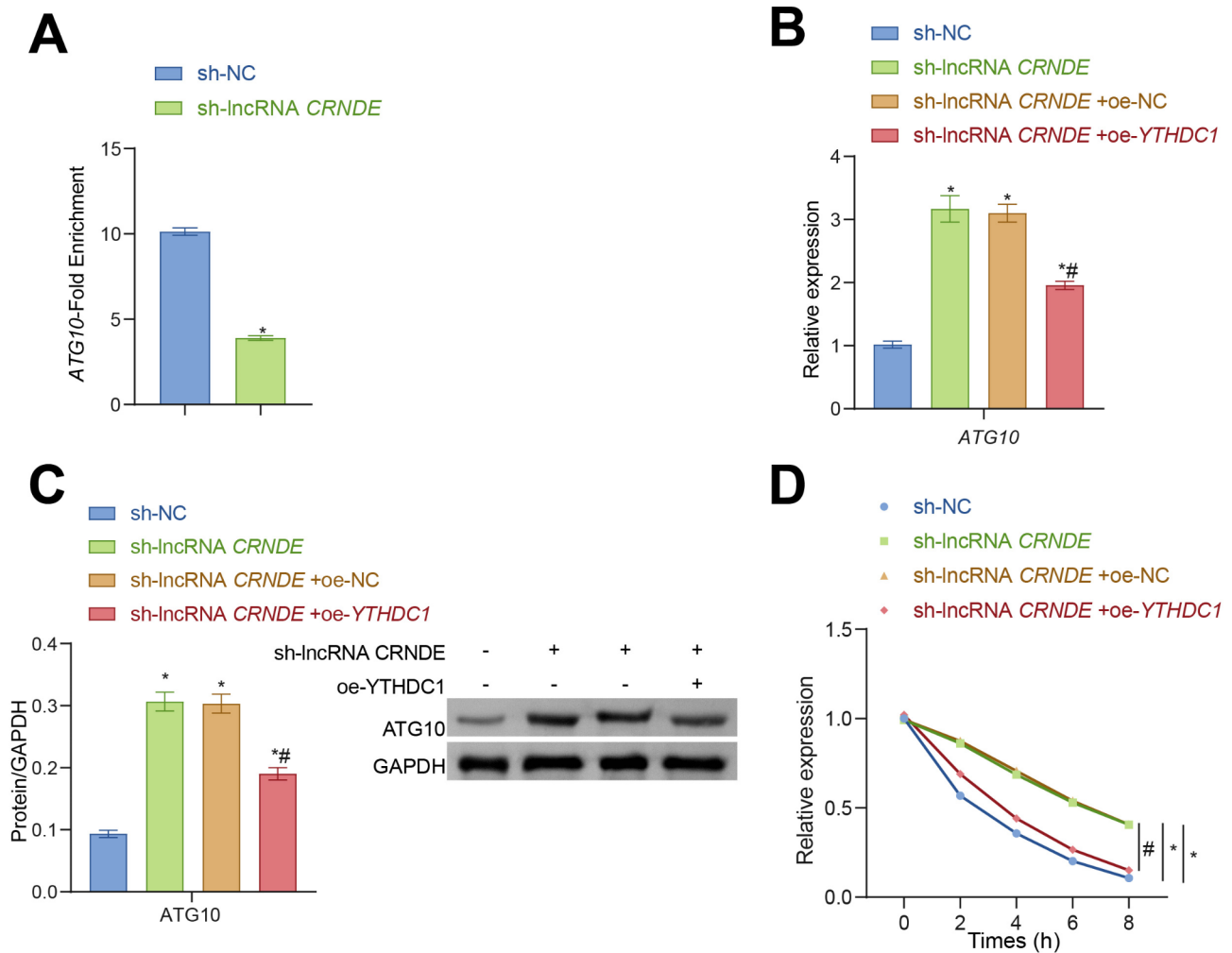


**Fig. 5** Overexpression of *YTHDC1* promotes *ATG10* expression. (**A**) RIP assay revealed a reduction in ATG10 expression upon inhibition of lncRNA CRNDE. (**B**) qRT-PCR analysis of *ATG10* mRNA levels. (**C**) Western blot analysis of ATG10 protein levels. (**D**) RNA stability assay in neuroblastoma cells treated with actinomycin. *$P < 0.05$ indicates a significant difference compared to the sh-NC group. #$P < 0.05$ indicates a significant difference compared to the sh-lncRNA *CRNDE* + oe-NC group. All data are expressed as Mean ± SD. Comparisons between two groups were performed using the unpaired Student's t-test, while one-way ANOVA and Tukey's post-hoc test were used for comparisons among multiple groups. All the experiments were repeated thrice

**Fig. 6** (See legend on next page.)

(See figure on previous page.)

**Fig. 6** METTL3 mediates lncRNA *CRNDE* m6A modification to inhibit OGD/R-induced neuronal cell apoptosis. (**A**) m6A quantification assay to determine m6A levels in cells and brain injury tissues. (**B**) MeRIP assay to measure m6A modification levels of lncRNA *CRNDE* in cells and brain injury tissues. (**C**) RIP assay to detect lncRNA *CRNDE* precipitation. (**D**) MeRIP analysis of m6A modification levels of lncRNA *CRNDE*. (**E**) Expression levels of *METTL3* and lncRNA *CRNDE*. (**F**) Flow cytometry analysis of apoptosis rate. (**G**) Western blot analysis of Bcl-2, Bax, and Caspase-3 proteins. (**H**) ELISA measurement of inflammatory factors TNF-α, IL-1β, IL-6, and IL-10. (**I**) qRT-PCR analysis of levels of *ATG10*, *LC3*, *Beclin1*, and *p62*. (**J**) Western blot analysis of ATG10, LC3II/I, Beclin1, and p62 proteins. *$P < 0.05$ indicates a significant difference compared to the oe-NC, Control, or Sham group. #$P < 0.05$ indicates a significant difference compared to the oe-*METTL3* + oe-NC group. All data are expressed as Mean ± SD. Comparisons between two groups were performed using the unpaired Student's t-test, while one-way ANOVA and Tukey's post-hoc test were used for comparisons among multiple groups. All the experiments were repeated thrice

demonstrated that ATG10 can promote tumor cell proliferation and malignant transformation. Conversely, downregulating p62 to suppress *ATG10*-mediated autophagy can worsen oxidative damage to the retinal pigment epithelium. Additionally, the upregulation of *ATG10* in neuroblastoma cells treated with MPP + has been shown to alleviate neuronal damage [38]. In our study, we successfully increased *ATG10* expression and enhanced autophagy in SH-SY5Y cells by overexpressing *METTL3* and silencing lncRNA *CRNDE*. However, the clinical implications of *ATG10* remain unexplored. Future research will focus on investigating the potential clinical applications of *ATG10*.

In conclusion, our study found that m6A levels were reduced in both the MCAO rat model and SH-SY5Y cells treated with OGD/R. Overexpression of the methyltransferase *METTL3* effectively inhibited lncRNA *CRNDE* expression. Inhibition of lncRNA CRNDE led to increased stability of ATG10 mRNA, which was reversed by YTHDC1. Silencing lncRNA *CRNDE* resulted in decreased apoptosis and enhanced autophagy in SH-SY5Y cells (Fig. 7). These findings suggest that lncRNA *CRNDE* holds potential therapeutic value for ischemia-reperfusion (I/R)-related diseases.
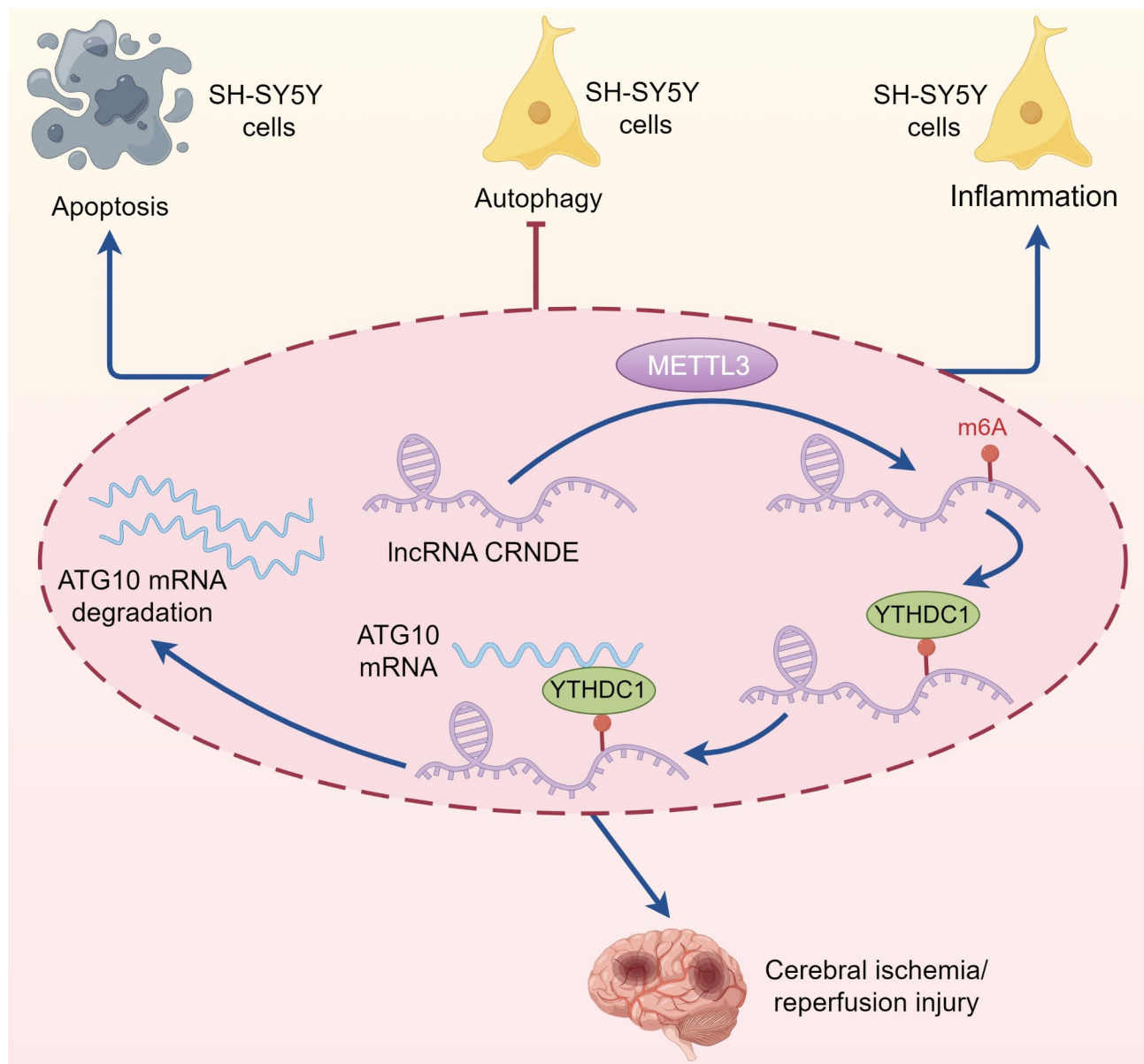
**Fig. 7** Graphic abstract of this study. Inhibiting lncRNA *CRNDE* expression reduces apoptosis, inhibits inflammatory factors, increases *ATG10* expression, and enhances autophagy

## Supplementary Information

The online version contains supplementary material available at https://doi.org/10.1186/s13062-024-00536-4.

Supplementary Material 1

### Author contributions
W.L. and YJ.L. designed experiments and directed the project. Z.Y., Y.X., L.L., J.J. and Y.L. performed experiments and collected the data. Z.Y. analyzed experiments and the data, and drafted the manuscript. All the authors reviewed the manuscript. All authors read and approved the final manuscript.

### Data availability
All data found in this study are included in this paper and are available on reasonable request.

## Declarations

### Conflict of interest
We declare that there are no conflicts of interest in this study.

## References

1. Si W, et al. Methyltransferase 3 mediated miRNA m6A methylation promotes stress granule formation in the early stage of Acute ischemic stroke. Front Mol Neurosci. 2020;13:103.
2. Lee WT, et al. YC–1 reduces inflammatory responses by inhibiting nuclear factor–κB translocation in mice subjected to transient focal cerebral ischemia. Mol Med Rep. 2018;18(2):2043–51.
3. Nogueira RG, et al. Thrombectomy 6 to 24 hours after stroke with a mismatch between Deficit and Infarct. N Engl J Med. 2018;378(1):11–21.
4. Li ZR, et al. Nobiletin protects PC12 cells from ERS-induced apoptosis in OGD/R injury via activation of the PI3K/AKT pathway. Exp Ther Med. 2018;16(2):1470–6.
5. Niu Y, et al. N6-methyl-adenosine (m6A) in RNA: an old modification with a novel epigenetic function. Genomics Proteom Bioinf. 2013;11(1):8–17.
6. Li Y, et al. The alteration profiles of m(6)A-Tagged circRNAs in the Peri-infarct Cortex after cerebral ischemia in mice. Front Neurosci. 2022;16:869081.
7. Xu K, et al. N(6)-methyladenosine demethylases Alkbh5/Fto regulate cerebral ischemia-reperfusion injury. Ther Adv Chronic Dis. 2020;11:2040622320916024.
8. Sheng Y, et al. A critical role of nuclear m6A reader YTHDC1 in leukemogenesis by regulating MCM complex-mediated DNA replication. Blood. 2021;138(26):2838–52.
9. Zhao X, et al. FTO-dependent demethylation of N6-methyladenosine regulates mRNA splicing and is required for adipogenesis. Cell Res. 2014;24(12):1403–19.
10. Zhang Z, et al. YTHDC1 mitigates ischemic stroke by promoting akt phosphorylation through destabilizing PTEN mRNA. Cell Death Dis. 2020;11(11):977.
11. Kopp F, Mendell JT. Functional classification and experimental dissection of long noncoding RNAs. Cell. 2018;172(3):393–407.
12. Wang LK, et al. Dissection of functional lncRNAs in Alzheimer's disease by construction and analysis of lncRNA-mRNA networks based on competitive endogenous RNAs. Biochem Biophys Res Commun. 2017;485(3):569–76.
13. Choe HK, Cho J. Comprehensive genome-wide approaches to activity-dependent translational control in neurons. Int J Mol Sci, 2020. 21(5).
14. Yao W, et al. N(6)-methyladenosine (m(6)A) methylation in ischemia-reperfusion injury. Cell Death Dis. 2020;11(6):478.
15. Xu S, et al. Oxygen glucose deprivation/re-oxygenation-induced neuronal cell death is associated with Lnc-D63785 m6A methylation and miR-422a accumulation. Cell Death Dis. 2020;11(9):816.
16. Chen J, et al. YTH domain family 2 orchestrates epithelial-mesenchymal transition/proliferation dichotomy in pancreatic cancer cells. Cell Cycle. 2017;16(23):2259–71.
17. Tandel P, et al. Decreased expression of autophagy-related genes in the complete remission phase of acute myeloid leukemia. Mol Genet Genomic Med. 2022;10(3):e1872.
18. Chun Y, Kim J. Autophagy: an Essential Degradation Program for Cellular Homeostasis and Life. Cells, 2018. 7(12).
19. Huang Q, et al. Autophagy core protein ATG5 is required for elongating spermatid development, sperm individualization and normal fertility in male mice. Autophagy. 2021;17(7):1753–67.
20. Noda NN, Inagaki F. Mech Autophagy Annu Rev Biophys. 2015;44:101–22.
21. Katsuragi Y, Ichimura Y, Komatsu M. p62/SQSTM1 functions as a signaling hub and an autophagy adaptor. Febs j. 2015;282(24):4672–8.
22. Yu L, et al. Formononetin protects against inflammation associated with cerebral ischemia-reperfusion injury in rats by targeting the JAK2/STAT3 signaling pathway. Biomed Pharmacother. 2022;149:112836.
23. Wang L, et al. ATP2B1-AS1 promotes cerebral Ischemia/Reperfusion Injury through regulating the miR-330-5p/TLR4-MyD88-NF-κB signaling pathway. Front Cell Dev Biol. 2021;9:720468.
24. Guo Y, et al. Protocatechuic aldehyde prevents ischemic injury by attenuating brain microvascular endothelial cell pyroptosis via lncRNA Xist. Phytomedicine. 2022;94:153849.
25. Min J, et al. Butylphthalide improves brain damage induced by renal ischemia-reperfusion injury rats through Nrf2/HO-1 and NOD2/MAPK/NF-κB pathways. Ren Fail. 2023;45(2):2259234.
26. Zhang Y, et al. The long noncoding RNA lncCIRBIL disrupts the nuclear translocation of Bclaf1 alleviating cardiac ischemia-reperfusion injury. Nat Commun. 2021;12(1):522.
27. Fu CH, et al. Silencing of long non-coding RNA CRNDE promotes autophagy and alleviates neonatal hypoxic-ischemic brain damage in rats. Mol Cell Biochem. 2020;472(1–2):1–8.
28. Sun TT, et al. Regulatory effect of long-stranded non-coding RNA-CRNDE on neurodegeneration during retinal ischemia-reperfusion. Heliyon. 2022;8(10):e10994.
29. Meyer KD, Jaffrey SR. The dynamic epitranscriptome: N6-methyladenosine and gene expression control. Nat Rev Mol Cell Biol. 2014;15(5):313–26.
30. Gu X, et al. N6-methyladenosine demethylase FTO promotes M1 and M2 macrophage activation. Cell Signal. 2020;69:109553.
31. Anders M, et al. Dynamic m(6)a methylation facilitates mRNA triaging to stress granules. Life Sci Alliance. 2018;1(4):e201800113.
32. Yu T, et al. Fusobacterium nucleatum promotes Chemoresistance to Colorectal Cancer by modulating Autophagy. Cell. 2017;170(3):548–e56316.
33. Lin KC, et al. Graphene oxide sensitizes cancer cells to chemotherapeutics by inducing early autophagy events, promoting nuclear trafficking and necrosis. Theranostics. 2018;8(9):2477–87.
34. Wang Y, et al. Significantly enhanced tumor cellular and lysosomal hydroxychloroquine delivery by smart liposomes for optimal autophagy inhibition and improved antitumor efficiency with liposomal doxorubicin. Autophagy. 2016;12(6):949–62.
35. Ji J, et al. XIAP limits autophagic degradation of Sox2 and is a therapeutic target in nasopharyngeal carcinoma stem cells. Theranostics. 2018;8(6):1494–510.
36. Jo YK, et al. Increased expression of ATG10 in colorectal cancer is associated with lymphovascular invasion and lymph node metastasis. PLoS ONE. 2012;7(12):e52705.
37. Xie K, et al. Role of ATG10 expression quantitative trait loci in non-small cell lung cancer survival. Int J Cancer. 2016;139(7):1564–73.
38. Zhao J, Li H, Chang N. LncRNA HOTAIR promotes MPP+-induced neuronal injury in Parkinson's disease by regulating the miR-874-5p/ATG10 axis. Excli j. 2020;19:1141–53.

## Publisher's note